Iraqi Journal of Physics, 2019 *Vol.17, No.41, PP. 29-39*
DOI: 10.20723/ijp.17.41.29-39

Synthesis and characterization of Iron tungstate oxide films by advanced controlled spray pyrolysis technique

Alaa A. Abdul-hamead, Zena A. Salman, Farhad M. Othman

Materials Engineering Departments, University of Technology, Baghdad, Iraq

E-mail: adr.alaaa@gmail.com

Abstract

For the first time Iron tungstate semiconductor oxides films ($FeWO_4$) was successfully synthesized simply by advanced controlled chemical spray pyrolysis technique, via employed double nozzle instead of single nozzle using tungstic acid and iron nitrate solutions at three different compositions and spray separately at same time on heated silicone (n-type) substrate at 600 °C, followed by annealing treatment for one hour at 500 °C. The crystal structure, microstructure and morphology properties of prepared films were studied by X-ray diffraction analysis (XRD), electron Scanning Electron Microscopy (SEM) and Atomic Force Microscopy (AFM) respectively. According to characterization techniques, a material of well-crystallized monoclinic phase $FeWO_4$ films with spindle and aggregated fine plates microstructures were obtained from using this advance technique, with thickness about 500 nm. Such these structures have been recognized as one of the most efficient microstructures due to their large specific surface area especially in gas sensor applications.

Key words
$FeWO_4$, semiconductor oxides, thin film, advance spray pyrolysis method, microstructure characterization.

Article info.
Received: Nov. 2018
Accepted: Dec. 2018
Published: Jun. 2019

تحضير وتشخيص أغشية اوكسيد تنغستات الحديد بواسطة تقنية الرش الحراري الكيميائي المطورة المسيطر عليها

الآء علاء الدين عبد الحميد، زينة عبد الامير سلمان، فرهاد محمد عثمان

قسم هندسة المواد، الجامعة التكنولوجية، بغداد، العراق

الخلاصة

لاول مرة أغشية أوكسيد تنغستات الحديد الشبة موصلة ($FeWO_4$) حضرت بنجاح بواسطة استخدام تقنية الرش الكيميائي الحراري المحدثة المسيطر عليها ذلك باستخدام فوهة مزدوجة بدلا من فوهة واحدة حيث استعمل حامض التنغستن ونترات الحديد كمحاليل للرش بثلاث نسب مختلفة وتم رش المحاليل بصورة منفصلة على شريحة سيليكون نوع مانح مسخنة بدرجة حرارة 600 م°، يليها معاملة حرارية التلدين بدرجة حرارة 500 م° لمدة ساعة واحدة. خصائص التركيب البلوري والبنية المجهرية و طوبوغرافية السطح للطبقة المحضرة تم دراستها بواسطة حيود الاشعة السينية، مجهر المسح الالكتروني و مجهر القوة الذرية على التوالي. وفقا لتقنيات التشخيص تشير الى تكون اغشية متبلورة من ($FeWO_4$) على شكل صفائح ناعمة متجمعة ناتجه من استخدام هذه التقنية المطورة، مثل هذه البنية تم التعرف عليها باعتبارها واحدة من أكثر البنى المجهرية كفاءة لامتلاكها مساحة سطحية كبيرة خاصة في تطبيقات المتحسس الغازي.

Introduction

In the current years, tungsten compounds has been paid a lots interest because of their fantastic physical and chemical properties, Tungsten compounds such as, tungsten oxides, carbides, nitrides, sulfides, bronzes, tungstate, tungsten metal have

very wealthy chemistry materials, and they're all important commercial materials [1]. They can be utilized in catalysis, photograph catalysis, electrical applications, photovoltaic cells, humidity and gaseous detecting, smart home windows and different chromogenic fields, scientific and dental applications, refractory materials, hard metals, armor [1]. Binary combinations of oxides will modify and improved the characteristic of different oxides [2]. Mixed oxides can be classified into two categories: the main classification includes those that form particular chemicals component such as $ZnSnO_3$ and Zn_2SnO_4, this type is fascinating for gas sensing purposes an$_4$d in addition to for obvious conductive electrodes, the second classification fall those blended oxides that compose solid solutions e.g. SnO_2-TiO_2 system is an example of such behavior [3]. Iron tungstate (FeWO) is among the most encouraging oxide and its electronic and attractive properties have been concentrated to discover its ability applications [4], it is belong to a fascinating family of wolframite type materials which have highly potential and technological applications. $FeWO_4$ tungstate is well-known p-type semiconductors from experimental measurements with energy band gap 2.0 eV [5]. Fe_2WO_6 was found to be a p-type semiconductor with an energy gap of 1.68 eV. The chemical phase diagram of Fe_2WO_6 configuration is described by means of the existence of a number of polymorphic phases, that makes the selective preparation of Fe_2WO_6 non- insignificant, earlier structural examinations have imply that Fe_2WO_6 can found in three featured systems, relying on their preparation situations, labeled as α, β and γ Fe_2WO_6, these phases are typically affected by preparation temperature and could be stabilized as a characteristic of rising reaction temperatures, with ill-defined phase boundaries [6]. Recently, various morphologies of metal oxide semiconductor (MOS) nano-strcutures for example like wire, belt, and bar and tetra-units have been broadly explored for gas detecting applications. It is notable that the detecting property of these sensors emphatically depend on the microstructure and surface morphology of MOS particularly; 1D-dimensional nanostructures, for example, wires, belts and needles nanostructure that have obtained a great of attention in numerous synthesis and design of nanodevice [7]. It is important that the affectability of substance gas sensors is unequivocally influenced by the particular surface of detecting materials. A higher particular surface of a detecting material prompts higher sensor affectability. Subsequently, numerous systems have been received to build the particular surface of detecting films with fine structured, taking advantage of the large specific surface of fine structured materials [8]. Tungsten oxides and tungstate could be synthesis in many method points of view, e.g. spray pyrolysis, sol-gel or thermal evaporation and oxidation of tungsten metal. In spray pyrolysis method has been carried out to board range of preparation thin and thick layers. These layers were utilized in different equipment, for example, solar cells, sensors, and solid oxide fuel cells. The characteristics of deposited layer relay on the conditions of fabrication [9].

Therefore, we report a technique that could success-fully prepare $FeWO_4$ film by advanced controlled chemical spray pyrolysis technique, the suggest process is easy, rapid, clean and actively efficient for preparation of microcrystalline materials with controlled size and shape and high density of surface area, which are

suitable for technological applications such as gas sensor application.

Experimental

Materials and method

The iron tungstate oxides films prepared by advance controlled spray pyrolysis method using double nozzle by spray aqueous solutions of tungstic acid (H_2WO_4) and iron nitrate non-ahydrate ($Fe(NO_3)_3.9H_2O$) separately at same time with molarity (0.1 M) at three different composition are summarized in Table 1. The whole spray system is homemade consists of the following: heater and thermocouple (k-type), double nozzle 1mm diameter with valve, electrical timer, air compressor, electrical gas valve and connectors. The following relationship has been used to calculate the material mass [10]:

$$w = \frac{Mw \times M \times VL}{1000} \quad (1)$$

where:

M_w= Molecular weight of the material (gm/mol).

M = Molarity of the material (mol/L).

V_L= Volume of distilled water (ml).

W = Material mass (gm).

Table 1: Mixing percentages of salts.

Salts	Samples Mix %		
	S1	**S2**	**S3**
H_2WO_4	3	1	1
$Fe(NO_3)_3.9H_2O$	1	1	3

The salts were dissolved after knowing the molecular weights in a certain volume of distilled water and placed on the magnetic stirrer for 20 min until the solution get homogeneous and to ensure that the material is completely dissolved, then equal volumes of both the two solutions 20 ml sprayed on the heated silicone (n-type) substrates at 600 ˚C, which was measured using a thermocouple with the help of a digital multi-meter. The other parameters like pressure, spray rate and spray distance technique are summarized in Table 2. After the deposition, the prepared samples were annealed for one hour at 500 ˚C and let the samples cooling inside furnace. This step is done for improving the quality and crystalline structure of the thin films according to author [11].

Table 2: Process parameters.

Process Conditions	Value
Pressure	7 bar
Air flow rate	8 cm^3/sec
Spray distance	25 ±1 cm
Spray solution size	20 ml
Feeding rate	2.5 ml/min
Spatter number	20
Period between Spatter	1-2 min

Materials characterizations

The crystal structure and phase identification of the films after annealing were characterized by X-ray diffraction (XRD) inspection with radiation CuKα (λ=1.5406 ˚A), the microstructures of the samples were investigated by scanning electron microscopy (SEM) and the surface morphology of samples was observation by atomic force microscopy (AFM).

The thickness of films was measured by using the optical interferometer method. This method is based on interference of the light beam reflection from thin film surface and substrate bottom. He-Ne Laser (632 nm) is used and the thickness can be obtained by using the formula below [12], and was calculated to be approximately 500 nm.

$$T = \frac{\Delta X}{X} * \frac{\lambda}{2} \quad (2)$$

where:

T = Thickness of the film in (nm).

X = Width of fringe (cm).

ΔX=Distance between two fringes(cm).

λ = Length of wave of laser light (nm).

Results and discussion

Crystal structure characteristics

Figs.1-3 show the XRD patterns result for S1, S2 and S3 samples respectively. All of XRD spectrums could be indicated to highly crystallized monoclinic iron tungsten oxides $FeWO_4$ structure oriented (111) at 100%, that is match with JCPDS-PDF card file No. (46-1446), these findings confirm the formation of $FeWO_4$ corroborating to the results from XRD analysis. An investigation and examination of these data demonstrate that the relating values are predictable with results detailed by other authors [13, 14]. The sharp diffraction features suggest the crystalline nature of all the samples. An increase in diffraction intensity indicates an increase in the crystallinity, which can be attributed to the annealing of the samples. In Fig.1 WO_3 oxide observed, has a polycrystalline thin film with a hexagonal system oriented (200) at 100% was found due to high content of tungsten salt, which is match with the JCPDS-PDF card file No.(033-1387). In Fig.2 a ternary crystal phase appears, which was identified as β-Fe_2WO_6, monoclinic system showing reflection peak oriented (600) at 100% which is in agreement with JCPDS No. (048-0741), this ternary crystal phase appeared with increasing Fe content, and there is more peaks were observed of $FeWO_4$. In Fig.3 increasing iron salts lead to formation of iron oxide Fe_3O_4 has a polycrystalline thin film with a cubic system oriented (311) at 100% according to JCPDS No.(026-1136). No characteristic peak of impurity was detected on XRD patterns meaning that the materials exhibits a high degree of purity. Table3-5 show the results data of S1, S2 and S3 samples compared with the standard cards. The mean crystallite size of samples was calculated from X-ray line broadening analysis using the Scherrer equation [15]. The mean crystallite size of $FeWO_4$ was found to be approximately 30.6, 27.2 and 34.3 nm of S1, S2, and S3 samples respectively, and found to be 30.98, 26.01 and 31.45 nm of WO_3, Fe_2WO_6 and Fe_3O_4 of S1, S2, and S3 samples, respectively.

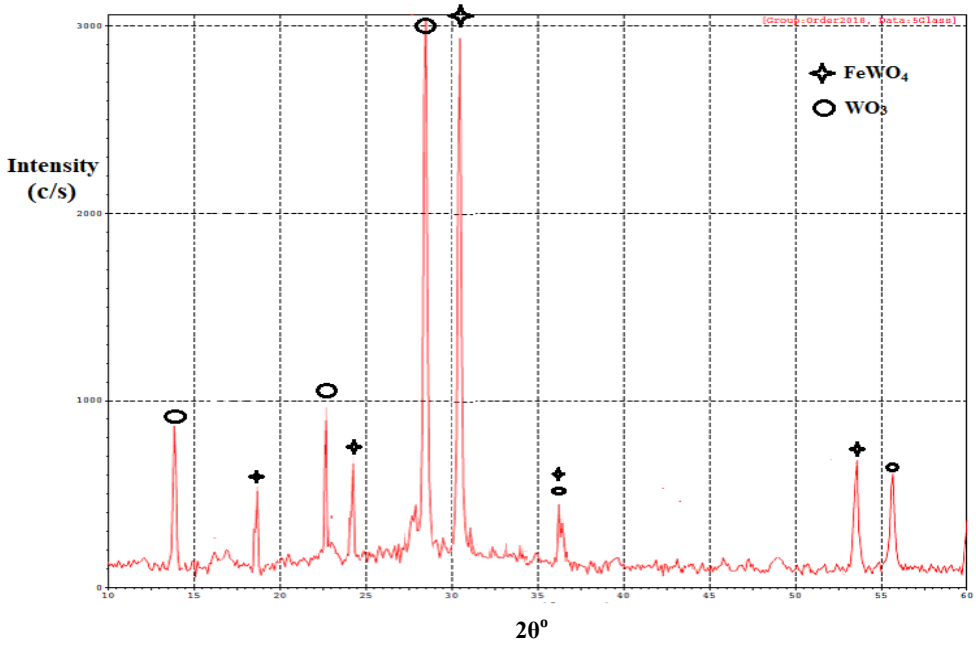

Fig. 1: XRD spectra of S1 sample.

Table 3: Results data of XRD S1 sample.

$FeWO_4$				WO_3			
2θ (deg.)	(hkl)	d(Å)	Intensity (c/s)	2θ (deg.)	(hkl)	d(Å)	Intensity (c/s)
18.660	100	4.465	20	13.956	100	5.959	30
24.360	110	3.432	30	22.716	001	3.677	30
30.360	111	2.763	100	28.150	200	2.977	100
36.230	021	2.329	20	36.550	201	2.309	20
53.455	221	1.609	30	55.525	221	1.554	25

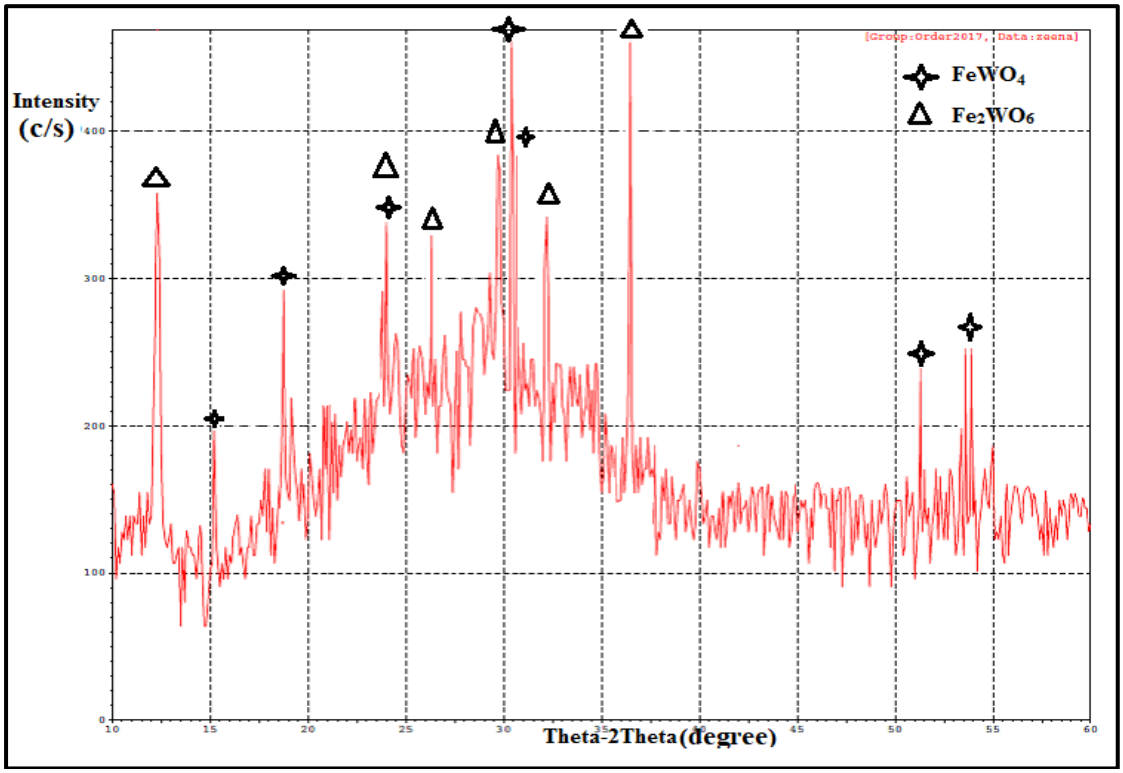

Fig. 2: XRD spectra of S2 sample.

Table 4: Results data of XRD S2 sample.

$FeWO_4$				Fe_2WO_6			
2θ(deg.)	hkl	d(Å)	Intensity (c/s)	2θ(deg.)	hkl	d(Å)	Intensity (c/s)
15.450	010	5.387	15	11.846	200	7.016	45
18.660	100	4.465	30	23.851	400	3.504	30
24.360	110	3.432	30	26.445	111	3.165	30
31.270	020	2.736	50	29.558	311	2.879	50
30.360	111	2.763	100	32.388	311	2.597	30
51.650	130	1.662	20	36.083	600	2.348	100
53.455	221	1.609	20				

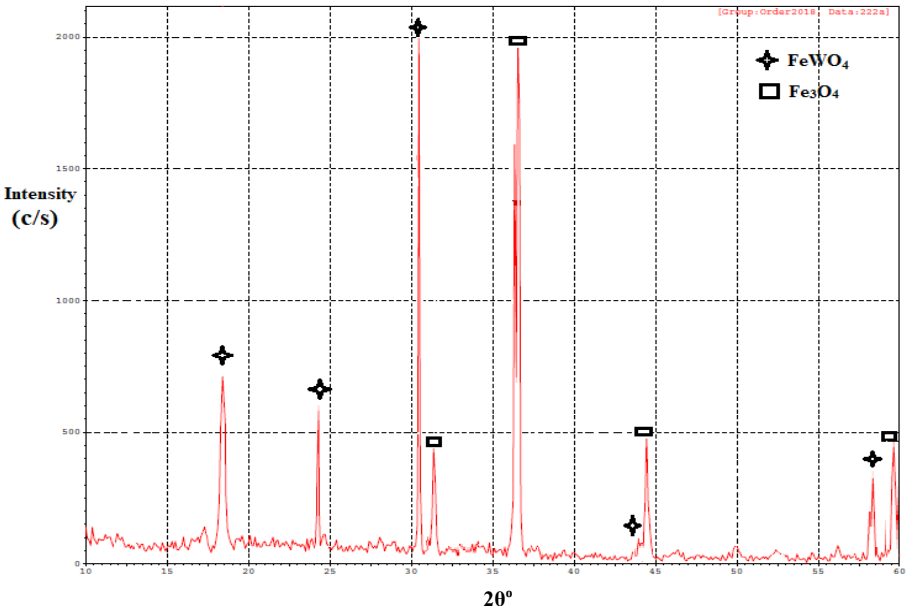

Fig. 3: XRD spectra of S3 sample.

Table 5: Results data of XRD S3 sample.

$FeWO_4$				Fe_3O_4			
2θ(deg.)	**hkl**	**d(Å)**	**Intensity (c/s)**	**2θ(deg.)**	**hkl**	**d(Å)**	**Intensity (c/s)**
18.660	100	4.465	30	31.259	220	2.688	25
24.360	110	3.432	25	36.811	311	2.295	100
30.360	111	2.763	100	44.752	400	1.903	30
44.1.50	112	1.961	10	59.321	511	1.464	30
53.455	221	1.609	20				

Microstructural and morphological characteristics (SEM & AFM)

The morphology of the prepared samples was studied by SEM, Figs.4-6 show microstructure photographs of annealed thin films deposited on silicon substrate. It is revealed that the prepared precipitate is well-crystalline formed under the current synthesis condition, which agrees well with the results of XRD. In Fig.4 shows a representative SEM image of $FeWO_4$ micro-plates in S1 which are found to be self-assembled to near micro-plates structures, high-magnification SEM images show that the $FeWO_4$ micro-plates have an about 4 µm length and 1-2 µm width and the films has a light brown color. In Fig. 5 was found high density of micro-plate and turn to be coarser, where the density and size of the micro-plates were found to increase with increasing iron precursor concentration, high-magnification SEM images show that the $FeWO_4$ micro-sheets have an about 5 µm length and 2 µm width and the films has a dark brown color due to high content of Fe. In Fig.6 the microstructure of $FeWO_4$ changed to be closer to smaller aggregated of uniform spindle structure with less dense and smoother comparing with S1 and S2 samples, it reveals a moderately smooth surface with irregular features, and the film become darker more. These microstructures possess high surface area, thus by using the advanced based system, micro crystallite sized thin films can be obtained.

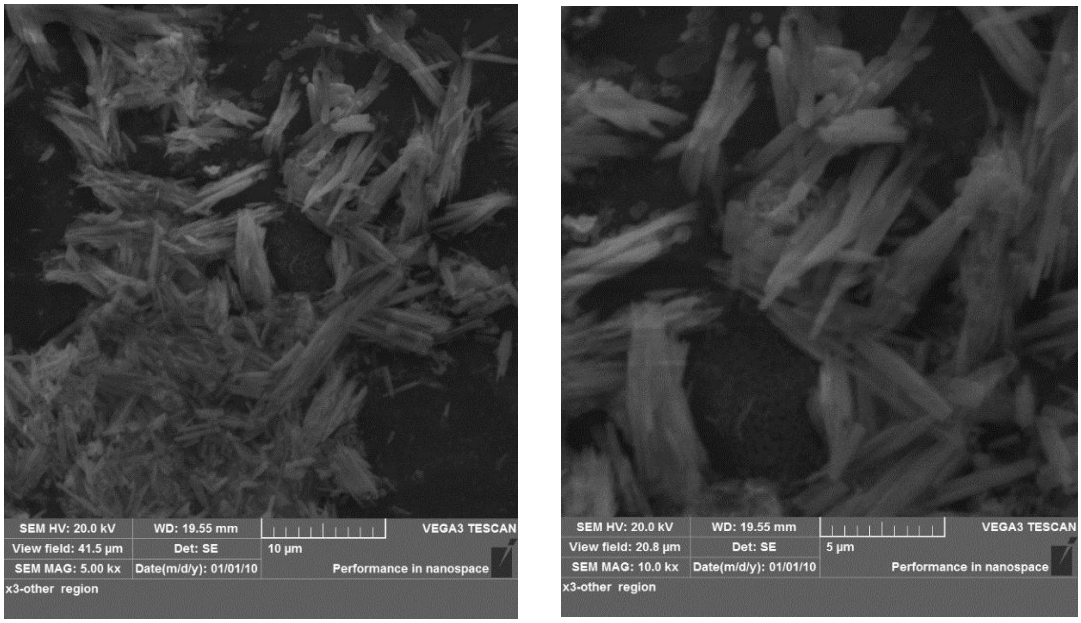

Fig. 4: SEM micrograph image for the S1 sample.

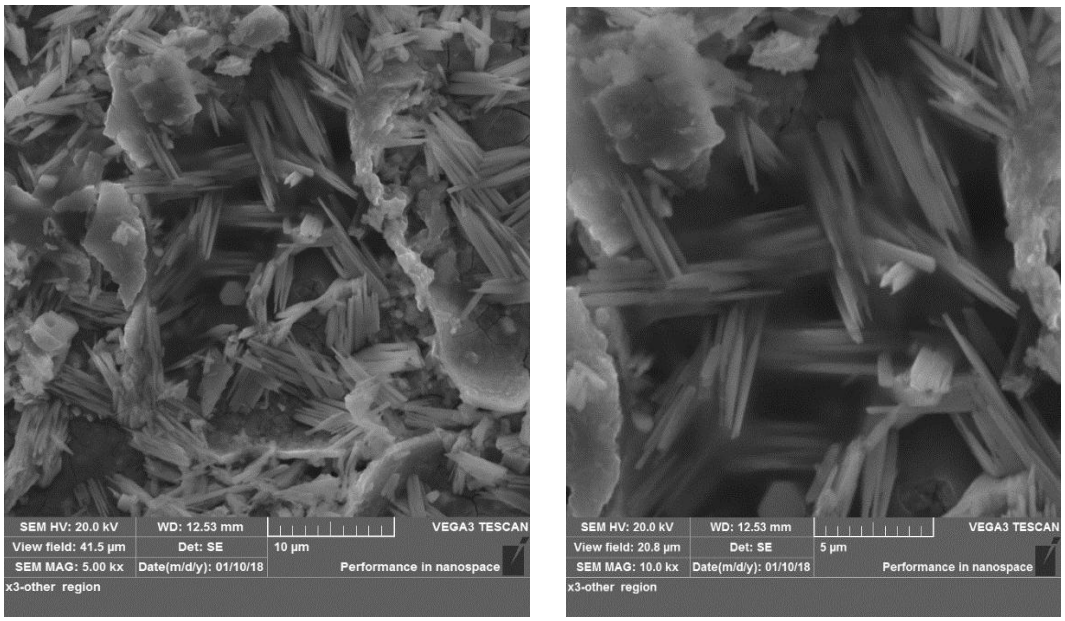

Fig. 5: SEM micrograph image for the S2 sample.

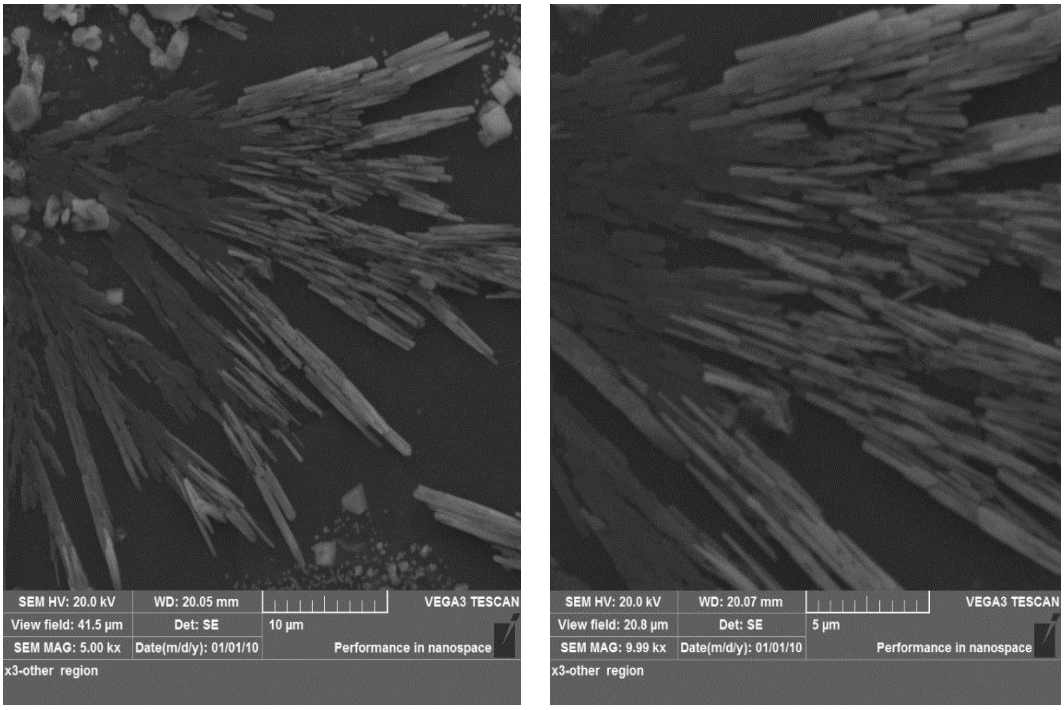

Fig. 6: SEM micrograph image for the S3 sample.

Figs.7-9 show AFM images of the surface topography of prepared films. As shown in granularity accumulation distribution chart of all samples have narrow range of diameter, it's observed that the average roughness decrease with increasing iron content and surface roughness average is small which shows very good smoothness of the surface and shows uniform surface. This means that the prepared films are well deposited. In Fig.7 the average roughness of S1 found to be 8.61 nm with average diameter 88.19 nm, and wide range of diameter comparing to S2 and S3 observed by granularity accumulation distribution chart. In Fig.8 average roughness of S2 found to be 1.39 nm with average diameter 79.76 nm, while in Fig. 9 average roughness of S3 found to be 0.6 nm with average diameter 68.12 nm, represent small roughness compared to S1 and S2.

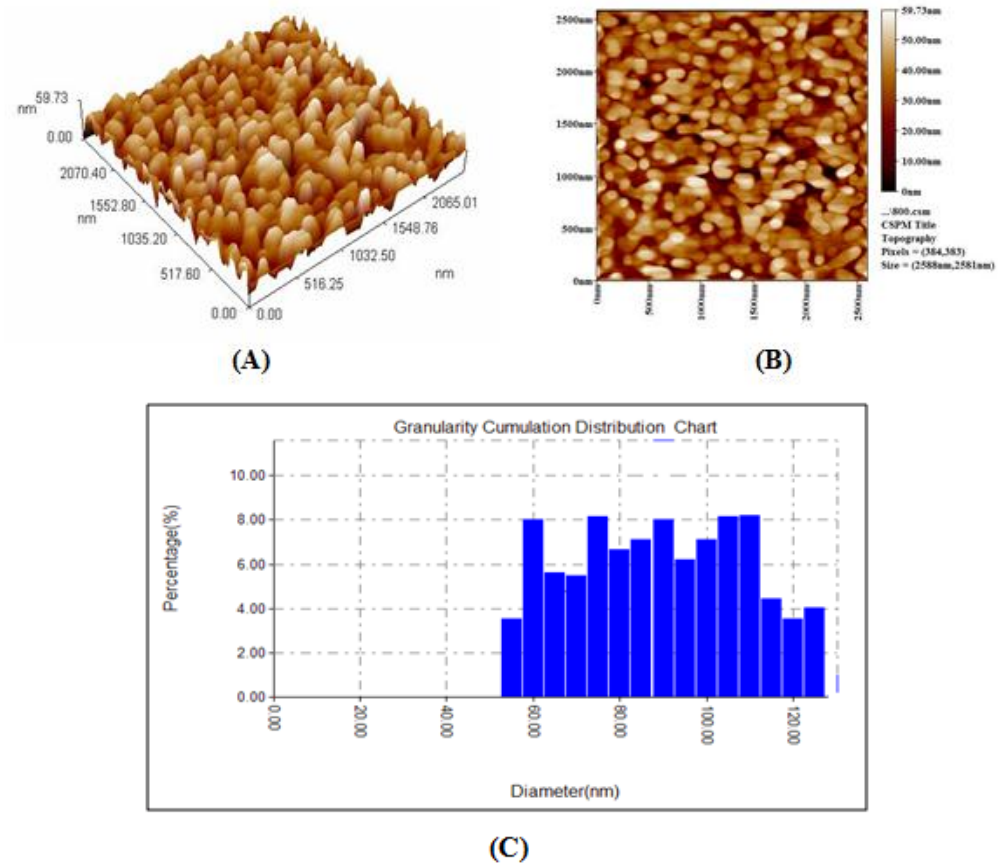

Fig. 7: AFM images (a) 3D and in (b) 2D and (c) Granularity accumulation distribution chart of the S1 sample.

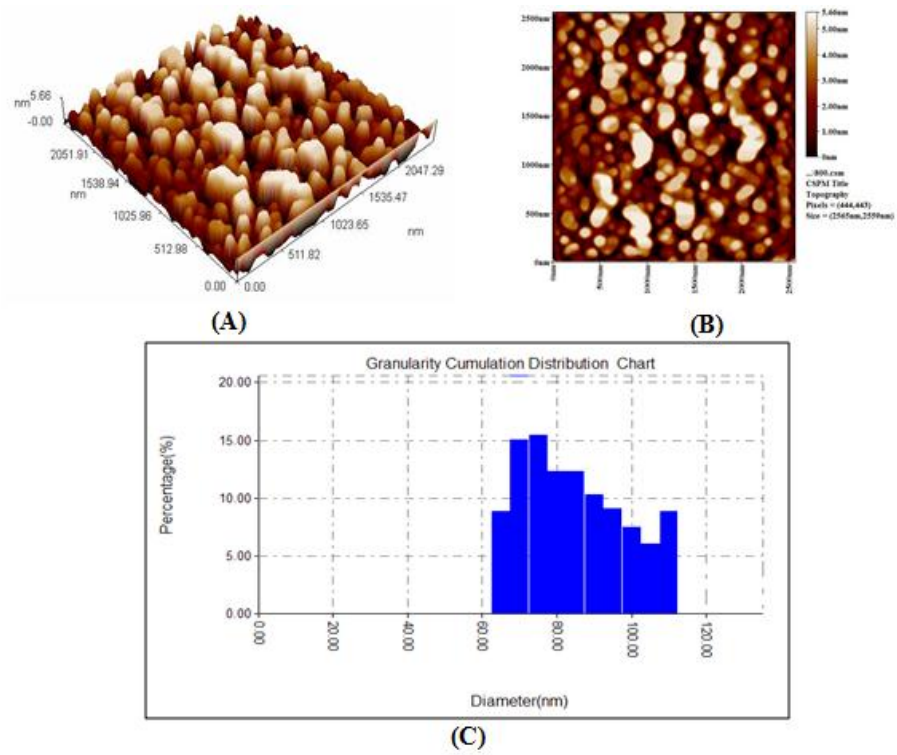

Fig. 8: AFM images (a) 3D and in (b) 2D and (c) Granularity accumulation distribution chart of the S2 sample.

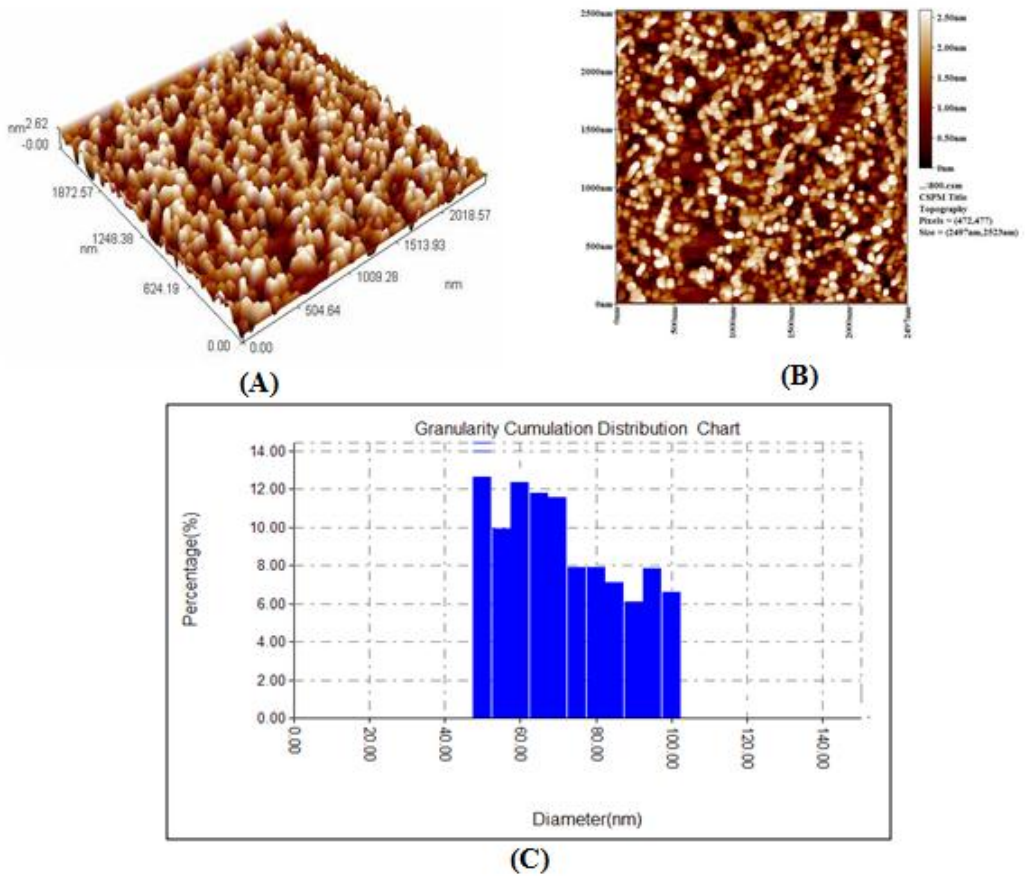

Fig. 9: AFM images (a) 3D and in (b) 2D and (c) Granularity accumulation distribution chart of the S3 sample.

Conclusions

1. It could conclude that the substrate temperature is suitable to obtain highly crystallized monoclinic iron tungsten film $FeWO_4$.
2. Spray pyrolysis technique using double nozzles offer different design to microstructure and this type is most efficient microstructures due to large specific surface area especially in gas sensor applications.
3. Decreased the tungsten salt content has changed the shape topography and microstructure of the films oxides, this is reflected in the changing proportions of the phases formed with different percentages of iron salt.

References

[1] T. N. Kovacs, G. Pokol, F. Gaber, D. Nagy, T. Igricz, I. E. Lukacs, Z. Fogarassy, K. Balazsi, I. M. Szilagyi: Mater. Res. Bull., 95 (2017) 563-569.

[2] A. A. Saad, S. Aly, M. A. Kaid., J. Mater Sci., 1 (2016) 10-19.

[3] K. Zakrzewska, Thin Solid Films, 391, 2 (2001) 229-238.

[4] M. A. P. Almeida, C. Morilla-Santos, L. S. Cavalcante, P. N. Lisboa Filho, A. Beltrán, J. Andrés, L. Gracia, E. Longo, J. A. Varela, Mater. Charact., 73 (2012) 124-129.

[5] S. Rajagopal, V.L. Bekenev, D. Nataraj, D. Mangalaraj, O.Yu. Khyzhun: J Alloy Comp., 496 (2010) 61-68.

[6] N. Guskos, L. Sadlowski, J. Typek, V. Likodimos, H. Gamari Seale, B. Bojanowski, M. Wabia, J. Walczak, I. Rychlowska-Himmel, J. Solid State Chem., 120, 2 (1995) 216-222.

[7] X. Peng: Nanowires - Recent Advances, InTech Publisher, Croatia (2012), Chap.1, p.3.
[8] B. Ding, M. Wang, J. Yu, G. Sun, AH S Sens., 9 (2009) 1609-1624.
[9] D. Perednis, "Thin film deposition by spray pyrolysis and the application in solid oxide fuel cells", Ph.D. Thesis, Swiss Federal Institute of Technology Zurich, Lithuania, (2003).
[10] G. Baysinger and L. I. Berger: CRC Handbook of Chemistry and Physics, 96th Edition, CRC publication, National Institute of Standards and Technology, (2003).
[11] N. V. Long, T. Teranishi, Y. Yang, C. M. Thi, Y. Cao, M. Nogami, Int. J. Metall Mater Eng., 1 (2015) 1-18.
[12] M. Hernández, A. Juárez, R. Hernández, Superficies y Vacío, 9 (1999) 283-285.
[13] X. Cao, Y. Chen, S. Jiao, Z. Fang, M. Xu, X. Liu, L. Li, G. Pang, S. Fenga, Roy. Soc. Ch., 6, 21 (2014) 12366-12370.
[14] J. Guo, X. Zhou, Y. Lu, X. Zhang, S. Kuang, W. Hou, J. Solid State Chem, 196 (2012) 550-556.
[15] S. L. Zhang, J. O. Lim, J. S. Huh, J. S. Noh, W. Lee, Curr Appl Phys, 13 (2013) 156-161.